Stanford Exploration Project, Report 100, June 1, 1999, pages 11–34

Stanford Exploration Project, Report 100, June 1, 1999, pages 11–34

Wave-equation migration velocity analysis

Biondo Biondi and Paul Sava[1]

keywords: *velocity,wave-equation, MVA*

ABSTRACT

In this report, we introduce a new wave-equation method of migration velocity analysis (MVA). The method is based on the linear relation that can be established between a perturbation in the migrated image and the generating perturbation in the slowness function. Our method consists of two steps: we first improve the focusing of the migrated image and then iteratively update the velocity model to explain the improvement in the focusing of the image. As a wave-equation method, our version of MVA is robust and generates smooth slowness functions without model regularization. We also show that our method has the potential to exploit the power of residual prestack migration to MVA.

INTRODUCTION

Seismic imaging is a two-step process: velocity estimation and migration. As the velocity function becomes more complex, the two steps become more and more dependent on each other. In complex depth-imaging problems, velocity estimation and migration are applied iteratively in a loop. To assure that this iterative imaging process converges to a satisfactory model, it is crucial that the migration and the velocity estimation are consistent with each other.

Kirchhoff migration often fails in complex areas, such as sub-salt, because the wavefield is severely distorted by lateral velocity variations, and thus complex multipathing occurs. As the shortcomings of Kirchhoff migration have become apparent (O'Brien and Etgen, 1998), there has been a renewal of interest in wave-equation migration and the development of computationally efficient 3-D prestack depth-migration methods based on the wave equation (Biondi and Palacharla, 1996; Biondi, 1997; Mosher et al., 1997). However, there has been no corresponding progress in the development of migration velocity analysis (MVA) methods that can be used in conjunction with wave-equation migration.

In this paper, we propose a method that aims to fill this gap and that, at least in principle, can be used in conjunction with any downward-continuation migration method. In particular, we have been applying our new methodology to downward continuation based on the Double

[1]**email:** biondo@sep.stanford.edu, paul@sep.stanford.edu

Square Root equation in two dimensions (Yilmaz, 1979; Claerbout, 1985; Popovici, 1996) and on common-azimuth continuation in three dimensions (Biondi and Palacharla, 1996).

As for migration, wave-equation MVA is intrinsically more robust than ray-based MVA, because it avoids the well-known problems that rays encounter when the velocity model is complex and has sharp boundaries. The transmission kinematic component of the finite-frequency wave propagation is mostly sensitive to smooth variations in the velocity model. Consequently, wave-equation MVA produces smooth velocity updates and is therefore stable. In most cases, no smoothing constraints are needed to assure stability in the inversion. In contrast, ray-based methods require strong smoothing constraints to avoid quick divergence.

Our method is closer to conventional MVA than other wave-equation methods that have been proposed to estimate the background velocity model (Noble et al., 1991; Bunks et al., 1995; Fogues et al., 1998), because it tries to maximize the quality of the migrated image rather than to match the recorded data. In this respect, our method is related to differential semblance optimization (DSO) (Symes and Carazzone, 1991) and multiple migration fitting (Chavent and Jacewitz, 1995). However, in contrast to these two methods, our method has the advantage of exploiting the power of residual prestack migration to speed up the convergence.

AN ALGORITHM FOR ESTIMATING VELOCITY

We estimate velocity by iteratively migrating the prestack data and looping through the following steps:

1. Downward continuation with current velocity,
2. Extraction of common-image gathers from prestack wavefields (Prucha et al., 1999),
3. Residual prestack migration of common-image gathers,
4. Estimation of image perturbation from the results of residual prestack migration, and
5. Estimation of velocity perturbation from image perturbations.

The core technical element of the method is the estimation of velocity perturbations from image perturbations. The next section presents the linear theory that enables us to achieve this goal.

LINEAR THEORY

In migration by downward continuation, illustrated in Figure 1, data measured at the surface (D) are recursively propagated down in depth to generate the complete wavefield (U). Downward continuation requires us to make an assumption about the magnitude of the slowness field (S). Once the wavefield is known, we can apply the imaging condition, which gives us the wavefield at time zero, or in the other words, the image or reflectivity map at the moment the reflectors explode (R).

In the presence of the background wavefield (U), a perturbation in slowness (ΔS) will generate a scattered wavefield (ΔW), which can, by the same method as the background field, be downward continued (ΔU) and imaged (ΔR), as shown in Figure 1.

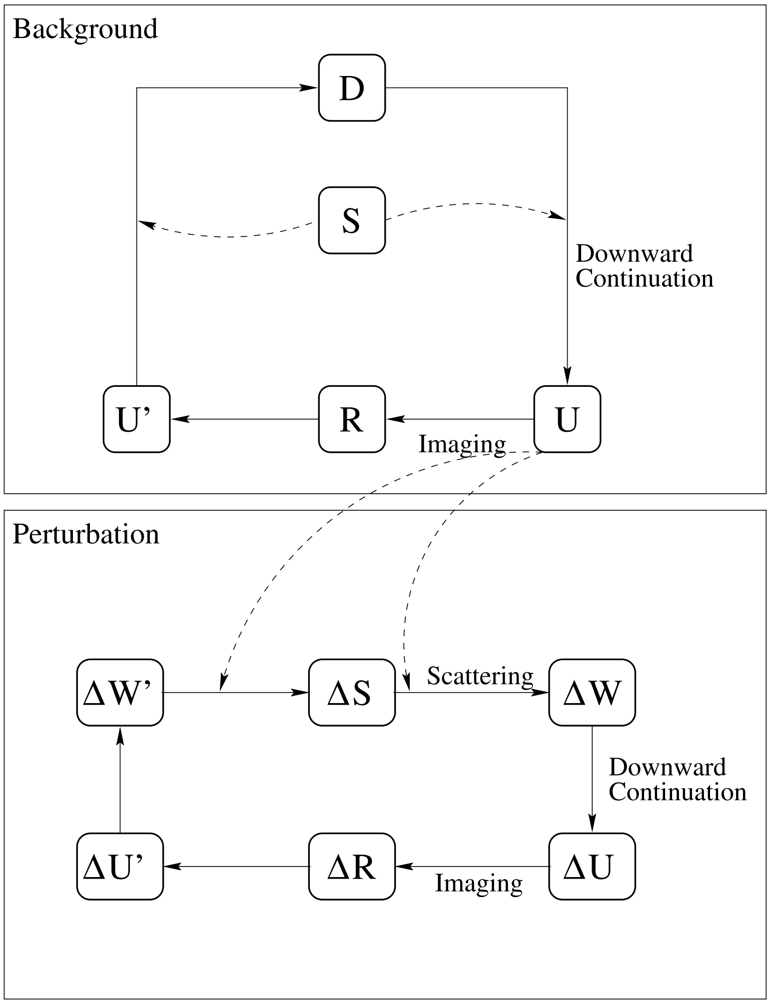

Figure 1: A summary-chart of our MVA method. The upper panel describes the computations done with respect to the background field, while the bottom panel refers to the computations done with respect to the perturbation field. biondo2-chart [NR]

We can take the perturbation in image (ΔR) and apply to it the adjoint operation. Doing so creates an adjoint perturbation in wavefield ($\Delta U'$), an adjoint scattered field ($\Delta W'$), and eventually an adjoint perturbation in slowness ($\Delta S'$), as the bottom panel of Figure 1 shows. Considering a first-order Born relation between the perturbation in slowness and the scattered wavefield, we can establish a direct linear relation between the perturbation in image (ΔR) and the perturbation in slowness (ΔS). It follows that if we can obtain a better focused image, we can iteratively invert for the perturbation in slowness that generated the improvement in focusing. This is the foundation of our wave-equation MVA method.

In the next two sections, we briefly present the mathematical relations that form the basis of our method. A more detailed mathematical description appears in Appendices A and B.

Background field: Forward operator

Migration by downward continuation, in post-stack or prestack, is done in two steps: the first step is to downward continue the data (D) measured at the surface, and the second is to apply the imaging condition, that is, to extract the wavefield at time $t = 0$, or the image (R) at the moment the reflectors explode (Claerbout, 1985).

1. Downward continuation

   The first step of migration consists of downward continuation of the wavefield measured at the surface (a.k.a. the data), which is done by the recursive application of the equation

   $$u_0^{z+1} = T_0^z u_0^z \tag{1}$$

   initialized by the wavefield at the surface

   $$u_0^1 = f \cdot d \tag{2}$$

   where

   - $u_0^z(\omega)$ is the wavefield $u_0(\omega)$ at depth z,
   - $u_0^1(\omega)$ is the wavefield $u_0(\omega)$ at the surface ($z = 0$),
   - $T_0^z(\omega, s_0)$ is the downward continuation operator at depth z,
   - $d(\omega)$ is the data, i.e., the wavefield at the surface, and
   - $f(\omega)$ is a frequency-dependent scale factor for the data.

2. Imaging

   The second step of the migration by downward continuation is imaging. According to the exploding reflector concept, the image is found by selecting the wavefield at time $t = 0$, or equivalently, by summing over the frequencies ω:

   $$r_0^z = \sum_1^{N_\omega} u_0^z(\omega) \tag{3}$$

   where

   - r_0^z is the image (reflectivity) corresponding to a given depth level z.

Perturbation field: Forward operator

If we perturb the velocity model, we also introduce a perturbation in the wavefield. In other words, the perturbation in slowness generates a secondary scattered wavefield.

1. Scattering and downward continuation

   If we consider the perturbation in the wavefield at the surface, we can recursively downward continue it, adding at every depth step the scattered wavefield:

   $$\Delta u^{z+1} = T_0^z \Delta u^z + \Delta v^{z+1} \tag{4}$$

   where

   - $\Delta u^z(\omega)$ is the perturbation in the wavefield generated by the perturbation in velocity and downward continued from the surface, and
   - $\Delta v^{z+1}(\omega)$ represents the scattered wavefield caused at depth level $z+1$ by the perturbation in velocity from depth level z.

   In the first-order Born approximation, the scattered wavefield can be written as

   $$\Delta v^{z+1} = T_0^z G_0^z u_0^z \Delta s^z \tag{5}$$

   where

   - $G_0^z(\omega, s_0)$ is the scattering operator at depth z,
   - $\Delta s^z(\omega)$ is the perturbation in slowness at depth z, and
   - $u_0^z(\omega)$ is the background wavefield at depth z.

   If we introduce equation (5) into (4) we find that

   $$\Delta u^{z+1} = T_0^z \left[\Delta u^z + G_0^z u_0^z \Delta s^z\right] \tag{6}$$

2. Imaging

   As for the background image, the perturbation in image (Δr^z), caused by the perturbation in slowness, is obtained by a summation over all the frequencies ω:

   $$\Delta r^z = \sum_1^{N_\omega} \Delta u^z(\omega) \tag{7}$$

Equations (6) and (7) establish a linear relation between the perturbation in slowness (Δs^z) and the perturbation in image (Δr^z). We can use this linear relation in an iterative algorithm to invert for the perturbation in slowness based on the perturbation in the image.

Perturbation field: Adjoint operator

In the adjoint operation, we begin by upward propagating the perturbation in wavefield at depth z:

$$\Delta u^{z-1} = T_0^{z'} \Delta u^z + \Delta r^{z-1} \tag{8}$$

where

- $T_0^{z'}$ is the upward continuation operator at depth z.

We can then obtain the perturbation in slowness from the perturbation in wavefield by applying the adjoint of the scattering operator:

$$\Delta s^z = u_0^{z'} G_0^{z'} \left[T_0^{z'} \Delta u^{z+1} - \Delta u^z \right] \tag{9}$$

Equations (6) and (7) for the forward operator and equations (8) and (9) for the adjoint operator express the linear relation established between the perturbation in slowness (ΔS) and the perturbation in image (ΔR).

AN EXAMPLE WITH SIMPLE REFLECTIVITY MODELS

This section offers a pictorial description of the theory presented in the preceding section. We use two simple examples to highlight the main features of the method. In both cases, the reflectivity model consists of two flat interfaces, one shallow and one deep. The velocity models are different as follows:

- In the first model, we started with a constant velocity background of 2 km/s, on which we superimposed a positive Gaussian perturbation with a magnitude of 0.25 km/s, as shown in the right panel of Figure 2.
- In the second model, we superimposed a negative Gaussian anomaly with the magnitude of 0.5 km/s on the background velocity (Figure 2), while the perturbation remained the same as in the first model (the right panel of Figure 2). The main purpose of selecting this second velocity model was to demonstrate the robustness of the forward and adjoint operators to triplications in the wavefield.

We started by creating the synthetic data (D) that correspond to each of the individual models (Figure 3). In the second case, the reflection from the deeper interface creates a triplication caused by the Gaussian anomaly in the background velocity. Then, we migrated the synthetic data using the correct velocity models in each case, and obtained the background images (R) shown in Figure 4.

We then repeated the same succession of operations, considering the background velocity models on which we superimposed the perturbation anomaly. We then created the data and migrated it with the perturbation in slowness. What we obtained is the perturbation in image

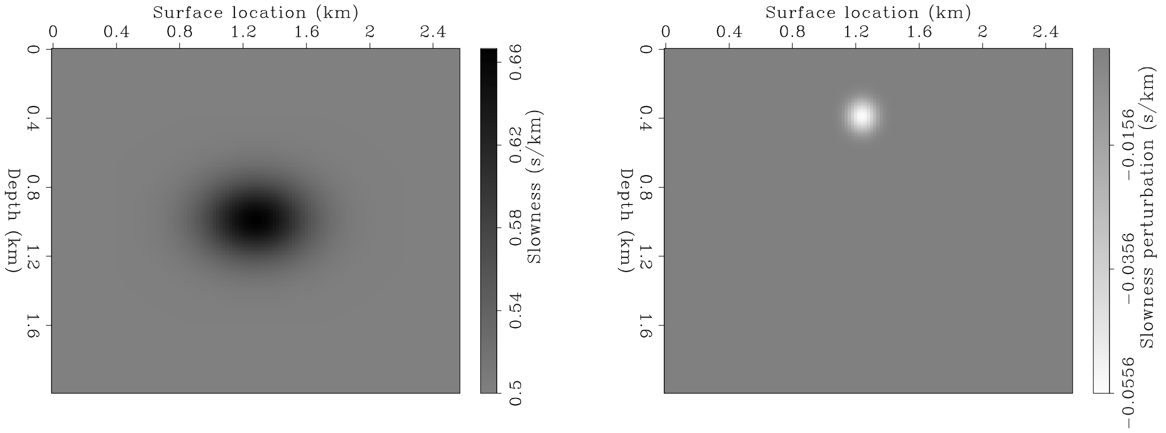

Figure 2: Background slowness (labeled S in Figure 1) – left; Perturbation in slowness (labeled ΔS in Figure 1) – right. biondo2-slow [NR]

depicted in Figure 5. The shape of the image at a given depth is known in the literature as *Kjartansson's V* (Kjartansson, 1979). In the case of the nonconstant background, the triplications of the wavefield created a more complex perturbation in the image, which is especially visible at the level of the deeper reflector. For this case, Kjartansson's V becomes a W (Figure 5).

Finally, we back-projected into the velocity model the perturbations we obtained in the images (Figure 6). To clarify how the back-projection operator works, we have isolated in each panel a single event of the perturbation in image, for a fixed reflection ray parameter. As expected, we have obtained "fat rays" showing which regions of the velocity model are influenced by the perturbation in image. The top panel of Figure 6 displays the straight fat rays corresponding to the constant velocity background. The bottom left panel, shows the rays for a similar perturbation in the image as in the first case, while the bottom right panel displays the rays for the perturbation in image in a region where the wavefield has triplicated when propagating through the anomaly in the background.

AN EXAMPLE OF INVERSION

This section presents an example inversion for the perturbation in slowness using the linear operators derived in the section on linear theory. For the inversion, we have created a set of synthetic data that was inspired by a real dataset, part of a gas-hydrate study, which was recorded at the Blake Outer Ridge, offshore from Florida and Georgia (Ecker, 1998). We have divided this example in two parts: in the first, we show how the focusing of the image can be improved, with application to the real data, and, in the second part, how the inversion works, with application to the smaller synthetic data set.

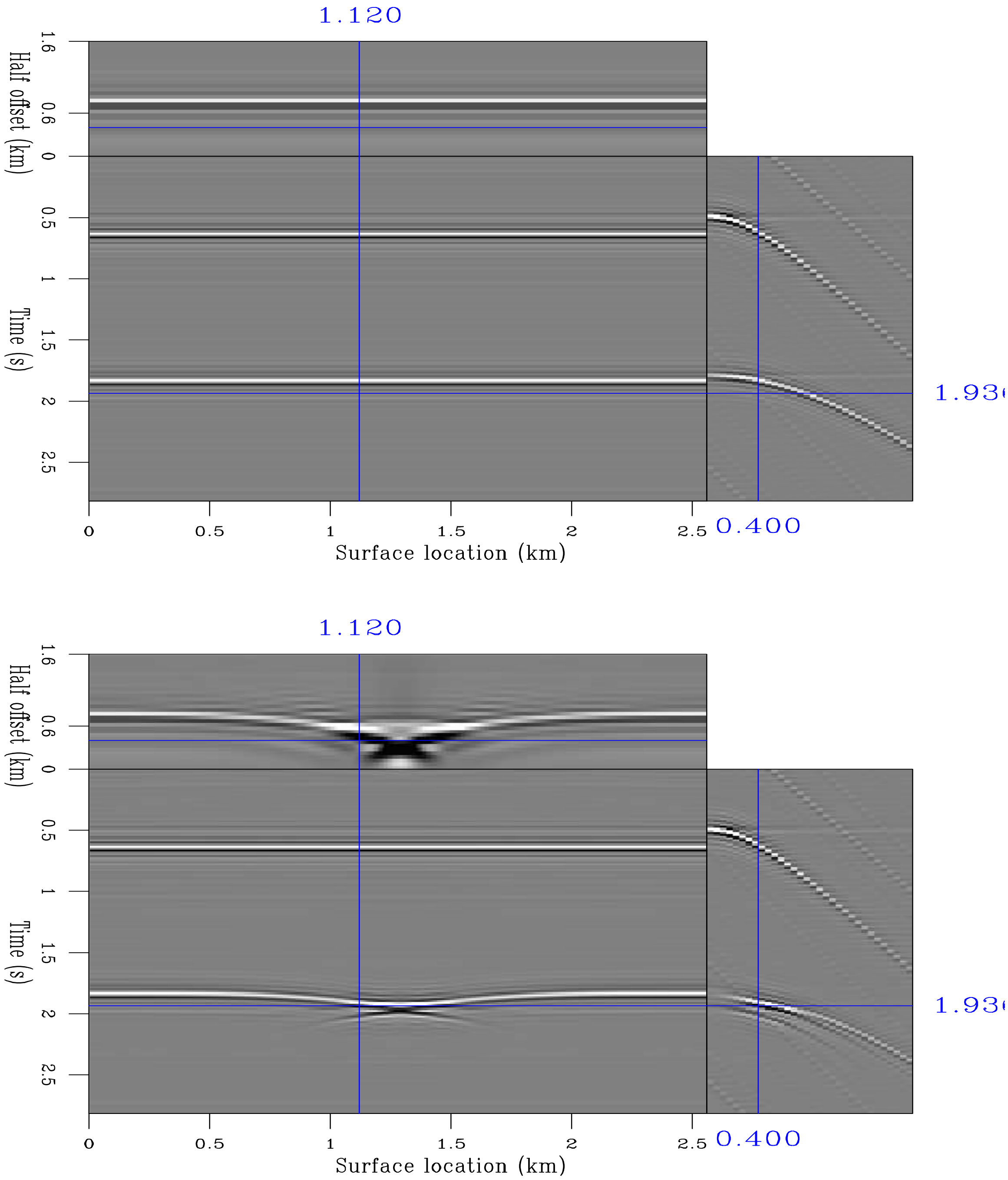

Figure 3: The data (labeled D in Figure 1) measured at the surface for each of the background velocity models. The top panel corresponds to the case of the constant background velocity, while the bottom panel corresponds to the case of the Gaussian anomaly in the background velocity. biondo2-data [CR]

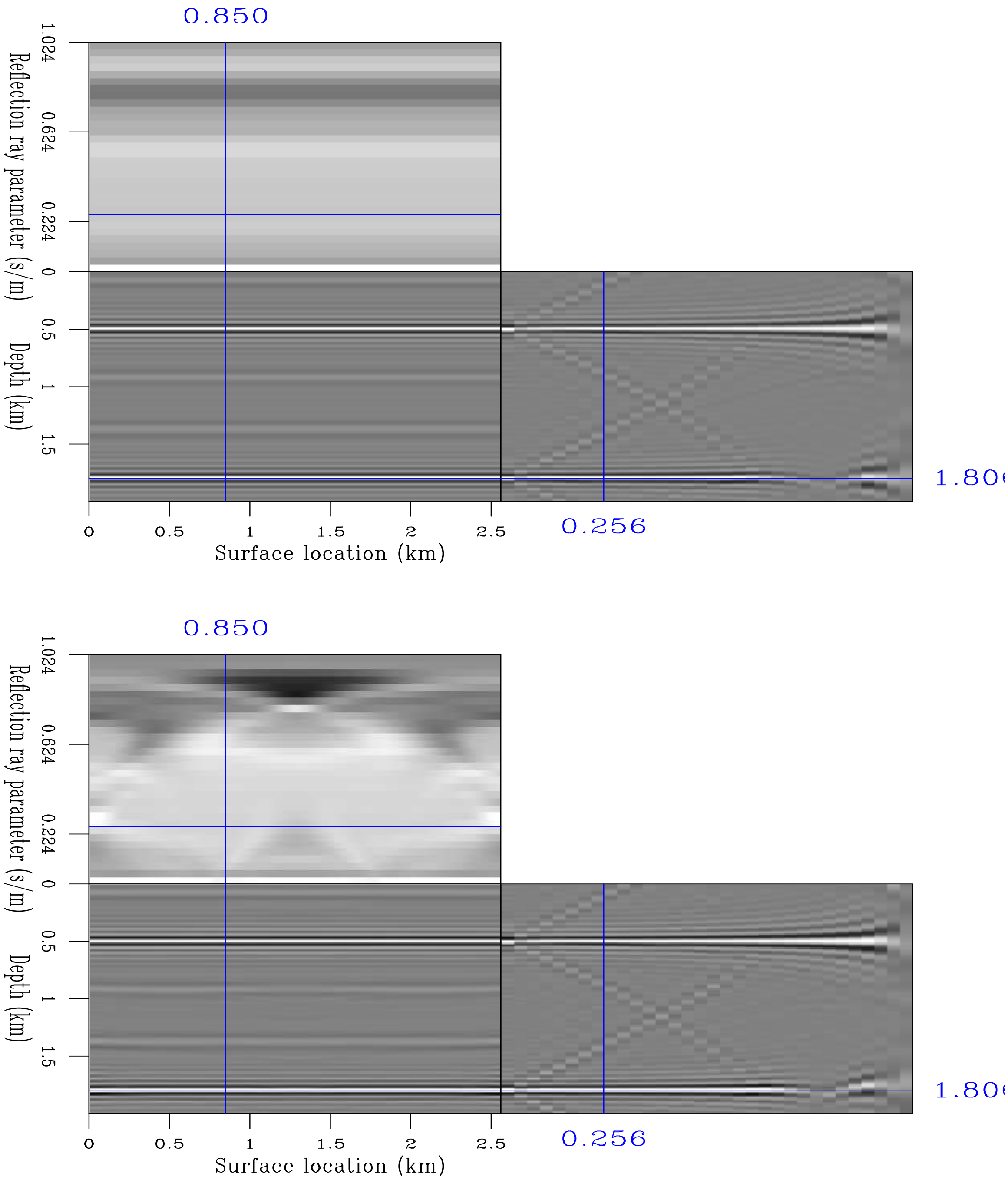

Figure 4: The image (labeled *R* in Figure 1) obtained after migrating by downward continuation the data in Figure 3. The top panel corresponds to the case of the constant background velocity, while the bottom panel corresponds to the case of the Gaussian anomaly in the background velocity. biondo2-image [CR]

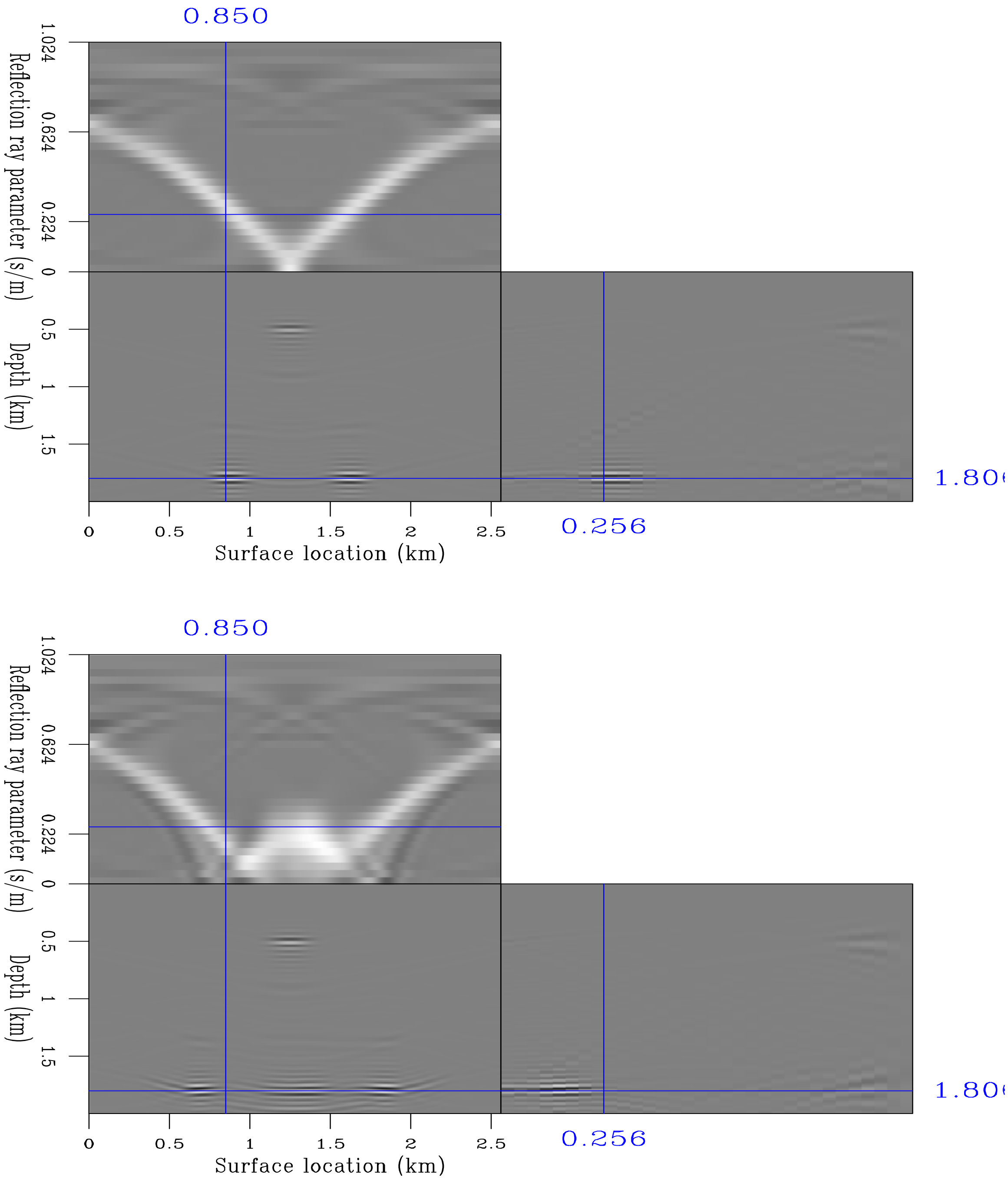

Figure 5: The perturbation in image (labeled ΔR in Figure 1), that is, the data migrated with the perturbation in slowness. The top panel corresponds to the case of the constant background velocity (Kjartansson's V), while the bottom panel corresponds to the case of the Gaussian anomaly in the background velocity. biondo2-dimage [CR]

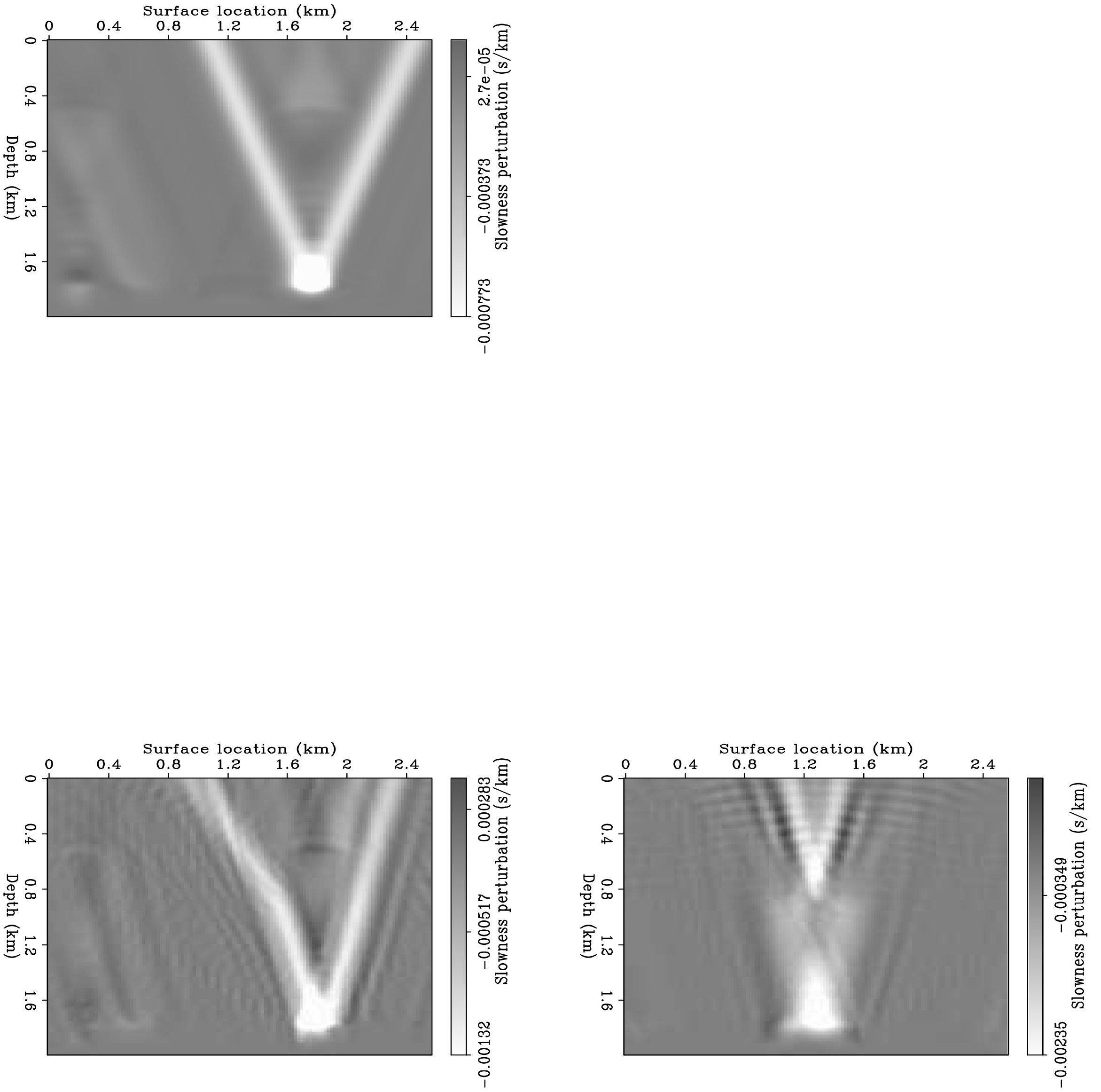

Figure 6: The perturbation in slowness (labeled ΔS in Figure 1) corresponding to part of the perturbation in image (Figure 5). The "fat rays" are the result of the back-projection of the perturbation in slowness. The top panel corresponds to the case of the constant background velocity, while the bottom panel corresponds to the case of the Gaussian anomaly in the background velocity. biondo2-rays [CR]

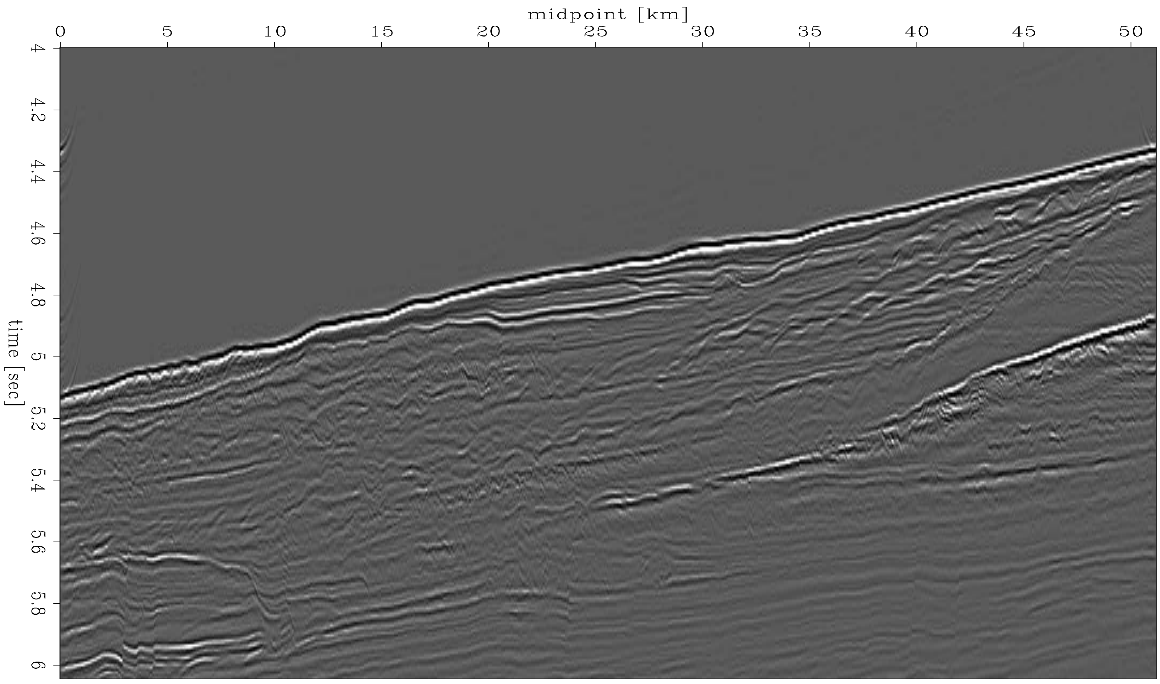

Figure 7: The original image.

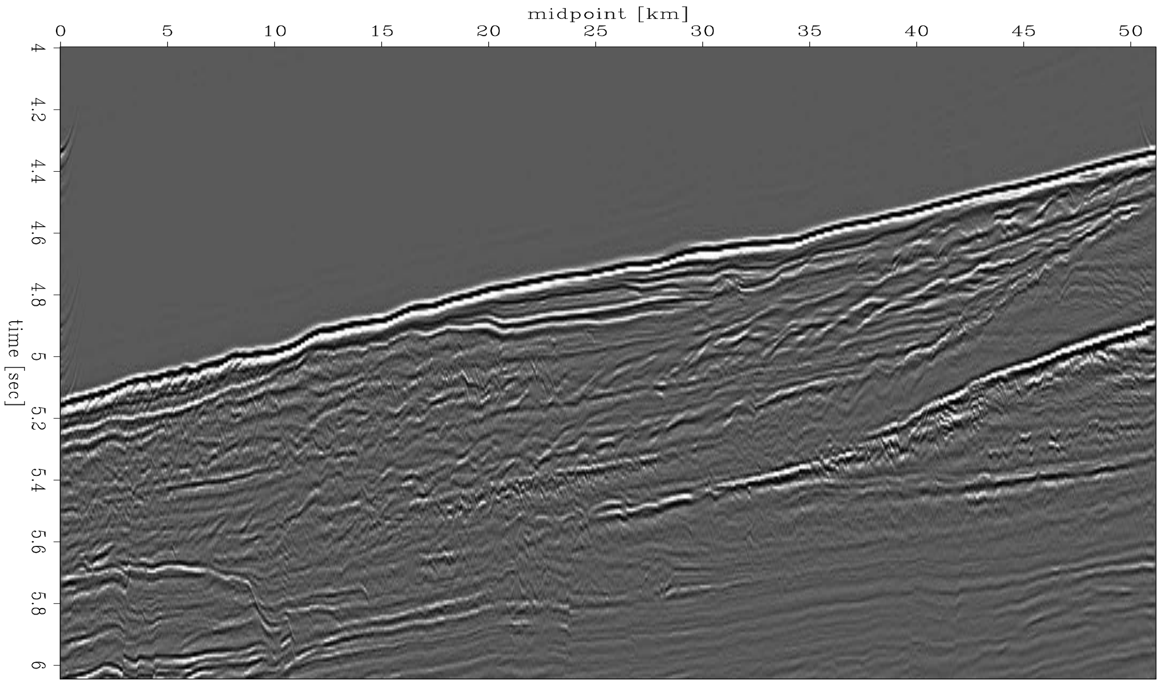

Figure 8: A better focused image after residual migration. biondo2-hydrates0.98 [NR]

Image enhancement

In the first part of our example, we have concentrated on improving the focusing of the image. We achieved this goal by using Stolt residual migration in the prestack domain (Stolt, 1996; Sava, 1999). Of course, Stolt residual migration is not the only possibility, another alternative being velocity continuation (Fomel, 1997).

Figure 7 shows the image we obtained with a starting velocity model, while Figure 8 displays the image we obtained by applying residual migration to the original. Both images have been created with the same level of clipping. The second image is clearly better focused. We can take the difference between the images in Figures 7 and 8 to be the perturbation in image (ΔR), and use it to invert for the slowness model that generated the improvement in focusing.

Inversion

As a first experiment, we have constructed a synthetic model similar to the sections in Figures 7 and 8. As we said, our goal is to convert the differences in focusing between the two images, or the perturbation in the image, into a better slowness model, that is, to find the perturbation in the slowness.

Figure 9 represents the background slowness model (S). We used this model to generate the synthetic data at the surface (S), and then to compute the background wavefield (U) and the background image (R).

The top panel of Figure 10 shows the perturbation in slowness (ΔS). We used this model to generate the scattered wavefield (ΔW), the perturbation wavefield (ΔU), and the perturbation in image (ΔR).

We start the inversion by assuming zero perturbation in slowness. The middle panel of Figure 10 represents the perturbation in slowness obtained at the first iteration. At this stage, we have obtained only a small perturbation in slowness, which is not totally concentrated at the right location. An important part of the energy of the section is spread, for example in the region around the midpoint $2.2-2.4$km and around the depth $1.3-1.4$km. This artifact is the result of the still imperfect definition of the slowness anomaly, possibly caused by the proximity of the edge.

By the 20^{th} iteration, shown in the bottom panel of Figure 10, the perturbation in slowness is much better shaped, and the artifact at depth is much weaker. Also, the absolute magnitude of the anomaly is getting very close to the correct value: $s_{max} = 0.088$ s/km for the original, and $s_{max} = 0.084$ s/km for the inversion at the 20^{th} iteration.

CONCLUSION

We have presented a recursive wave-equation method of migration velocity analysis operating in the image domain. Our method is based on linearization of the downward continuation

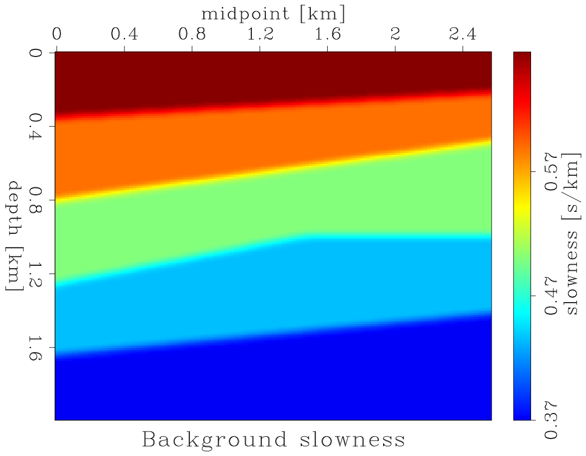

Figure 9: The background slowness (S). biondo2-backslo [NR]

operator that relates perturbations in slowness to perturbations in the image. The fundamental idea is to improve the quality of the slowness function by optimizing the focusing of the migrated image.

This iterative method is stable and accurate when applied to a synthetic dataset. It also converges to the solution without the need for any regularization of the slowness model. We are currently in the process of applying the method to the real seismic dataset used as an example in this paper.

REFERENCES

Biondi, B., and Palacharla, G., 1996, 3-D prestack migration of common-azimuth data: Geophysics, **61**, 1822–1832.

Biondi, B., 1997, Azimuth moveout + common-azimuth migration: Cost-effective prestack depth imaging of marine data: 67th Annual Internat. Mtg., Soc. Expl. Geophys., Expanded Abstracts, 1375–1378.

Bunks, C., Saleck, F. M., Zaleski, S., and Chavent, G., 1995, Multiscale seismic waveform inversion: Geophysics, **60**, no. 5, 1457–1473.

Chavent, G., and Jacewitz, C. A., 1995, Determination of background velocities by multiple migration fitting: Geophysics, **60**, no. 2, 476–490.

Claerbout, J. F., 1985, Imaging the Earth's Interior: Blackwell Scientific Publications.

Ecker, C., 1998, Seismic characterization of gas hydrates structures: Ph.D. thesis, Stanford University.

Fogues, E., Scala, E., and Pratt, R. G., 1998, High-resolution velocity estimation from refraction and reflection data: 68th Annual Internat. Mtg., Soc. Expl. Geophys., Expanded Abstracts, 1211–1214.

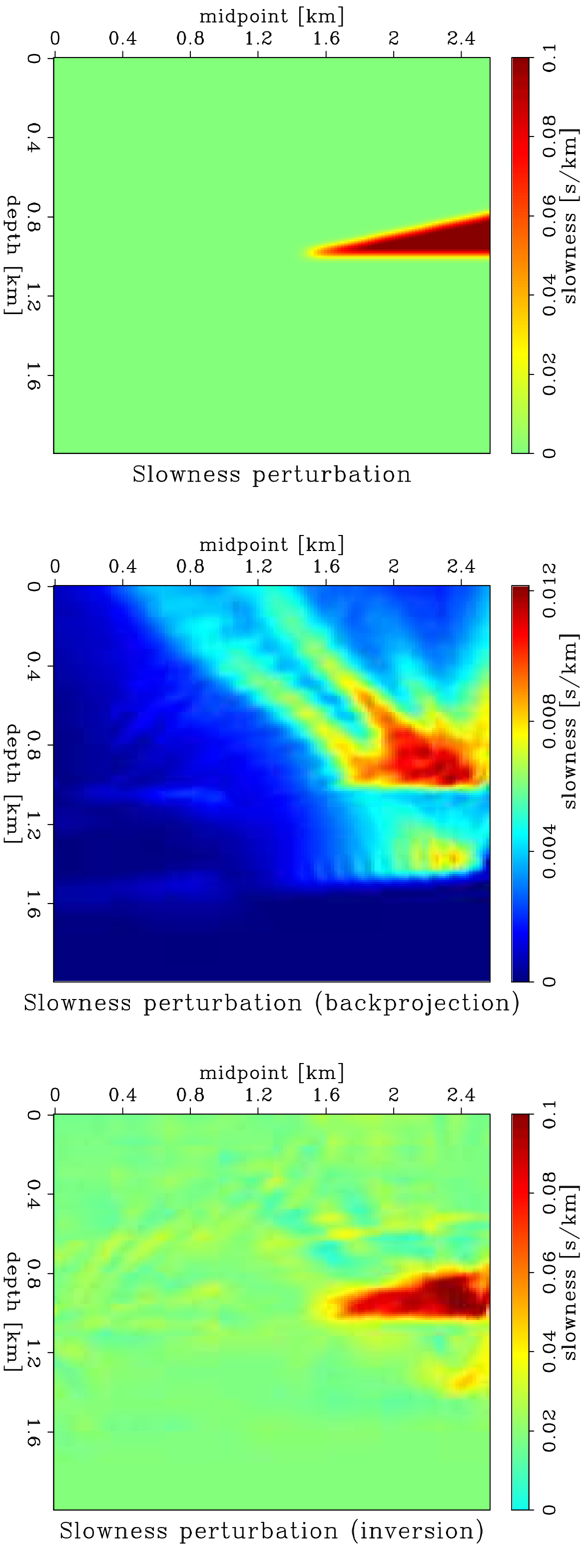

Figure 10: Top: the perturbation in slowness (ΔS). Middle: the perturbation recovered at the first iteration. Bottom: the perturbation recovered at the 20^{th} iteration. biondo2-inversion [CR]

Fomel, S., 1997, Velocity continuation and the anatomy of residual prestack migration: 67th Ann. Internat. Meeting, Soc. Expl. Geophys., 1762–1765.

Huang, L.-J., Fehler, M. C., and Wu, R.-S., 1999, Extended local Born Fourier migration method: submitted for publication to Geophysics.

Kjartansson, E., 1979, Attenuation of seismic waves in rocks and applications in energy exploration: Ph.D. thesis, Stanford University.

Mosher, C. C., Foster, D. J., and Hassanzadeh, S., 1997, Common angle imaging with offset plane waves: 67th Annual Internat. Mtg., Soc. Expl. Geophys., Expanded Abstracts, 1379–1382.

Noble, M., Lindgren, J., and Tarantola, A., 1991, Large-sized, nonlinear inversion of a marine data set: Retrieving the source, the background velocity and the impedance contrasts: 61th Annual Internat. Mtg., Soc. Expl. Geophys., Expanded Abstracts, 893–896.

O'Brien, M. J., and Etgen, J. T., 1998, Wavefield imaging of complex structures with sparse point-receiver data: 68th Annual Internat. Mtg., Soc. Expl. Geophys., Expanded Abstracts, 1365–1368.

Popovici, A. M., 1996, Short note–prestack migration by split-step DSR: Geophysics, **61**, no. 05, 1412–1416.

Prucha, M., Biondi, B., and Symes, W., 1999, Angle-domain common image gathers by wave-equation migration: 69th Annual Internat. Mtg., Soc. Expl. Geophys., Expanded Abstracts, submitted.

Sava, P., 1999, On Stolt prestack residual migration: SEP–**100**, 151–158.

Stolt, R. H., 1996, Short note–a prestack residual time migration operator: Geophysics, **61**, no. 02, 605–607.

Symes, W. W., and Carazzone, J. J., 1991, Velocity inversion by differential semblance optimization: Geophysics, **56**, no. 5, 654–663.

Yilmaz, O., 1979, Prestack partial migration: Ph.D. thesis, Stanford University.

APPENDIX A: DOWNWARD CONTINUATION–MIGRATION AND MODELING

Forward operator: Migration

Migration by downward continuation, either post-stack or prestack, is done in two steps: the first step is to downward continue the data measured at the surface, and the second is to apply the imaging condition, that is, to extract the wavefield at time $t = 0$, the moment the reflectors explode.

1. Downward continuation

   The first step of migration consists of downward continuation of the wavefield measured at the surface (a.k.a. the data), which is done by the recursive application of the equation:

$$\boxed{u_0^{z+1}(\omega) = T_0^z(\omega, s_0) u_0^z(\omega)} \tag{A-1}$$

   initialized by the wavefield at the surface, as follows:

$$u_0^1(\omega) = f(\omega) d(\omega) \tag{A-2}$$

   where

   - $u_0^z(\omega)$ is the wavefield $u_0(\omega)$ at depth z,
   - $u_0^1(\omega)$ is the wavefield $u_0(\omega)$ at the surface $z = 0$,
   - $T_0^z(\omega, s_0)$ is the downward continuation operator at depth z,
   - $d(\omega)$ is the data, i.e.. the wavefield at the surface, and
   - $f(\omega)$ is a frequency-dependent scale factor for the data.

   The recursion in Equations (A-1) and (A-2) can be also rewritten in matrix form as

$$\boxed{[\mathbf{I} - \mathbf{T_0}]\mathbf{U_0} = \mathbf{D}} \tag{A-3}$$

$$\begin{bmatrix} 1 & 0 & 0 & \dots & 0 & 0 \\ -T_0^1 & 1 & 0 & \dots & 0 & 0 \\ 0 & -T_0^2 & 1 & \dots & 0 & 0 \\ \dots & \dots & \dots & \dots & \dots & \dots \\ 0 & 0 & 0 & \dots & -T_0^{N_z-1} & 1 \end{bmatrix} \begin{bmatrix} u_0^1 \\ u_0^2 \\ u_0^3 \\ \dots \\ u_0^{N_z} \end{bmatrix} = \begin{bmatrix} f\,d \\ 0 \\ 0 \\ \dots \\ 0 \end{bmatrix}$$

   where

   - $\mathbf{T_0}$ is a square matrix containing the downward continuation operator for all depth levels,
   - $\mathbf{U_0}$ is a column vector containing the wavefield at all depth levels, and

- $\mathbf{D}$ is a column vector containing the scaled data. [2]

Equation (A-3) represents the downward continuation recursion written for a given frequency. We can write a similar relationship for each of the frequencies in the analyzed data, and group them all in the matrix relationship

$$\boxed{(\mathcal{I} - \mathcal{T}_0)\mathcal{U}_0 = \mathcal{D}} \tag{A-4}$$

$$\begin{pmatrix} \mathbf{I} - \mathbf{T_0}(\omega_1, \mathbf{s_0}) & 0 & \dots & 0 \\ 0 & \mathbf{I} - \mathbf{T_0}(\omega_2, \mathbf{s_0}) & \dots & 0 \\ \dots & \dots & \dots & \dots \\ 0 & 0 & \dots & \mathbf{I} - \mathbf{T_0}(\omega_{\mathbf{N}_\omega}, \mathbf{s_0}) \end{pmatrix} \begin{pmatrix} \mathbf{U_0}(\omega_1) \\ \mathbf{U_0}(\omega_2) \\ \dots \\ \mathbf{U_0}(\omega_{\mathbf{N}_\omega}) \end{pmatrix} = \begin{pmatrix} \mathbf{D}(\omega_1) \\ \mathbf{D}(\omega_2) \\ \dots \\ \mathbf{D}(\omega_{\mathbf{N}_\omega}) \end{pmatrix}$$

where

- $\mathcal{T}_0$ is a diagonal matrix containing the downward continuation operators for all the frequencies in the data,
- $\mathcal{U}_0$ is a column vector containing the wavefield data for all the frequencies, and
- $\mathcal{D}$ is a column vector containing the scaled data at all frequencies. [3]

It follows from Equation (A-4) that the background wavefield ($\mathcal{U}_0$) can be computed as a function of the measured data ($\mathcal{D}$), as follows:

$$\mathcal{U}_0 = (\mathcal{I} - \mathcal{T}_0)^{-1}\mathcal{D} \tag{A-5}$$

2. <u>Imaging</u>

   The second step of the migration by downward continuation is imaging. In the exploding reflector concept, the image is found by selecting the wavefield at time $t = 0$ or, equivalently, by summing over the frequencies ω:

$$\boxed{r_0^z = \sum_1^{N_\omega} u_0^z(\omega)} \tag{A-6}$$

where

- r_0^z is the image (reflectivity) corresponding to a given depth level z.

2

$$\mathbf{T_0}(\omega, \mathbf{s_0}) = \begin{bmatrix} 0 & 0 & 0 & \dots & 0 & 0 \\ T_0^1 & 0 & 0 & \dots & 0 & 0 \\ 0 & T_0^2 & 0 & \dots & 0 & 0 \\ \dots & \dots & \dots & \dots & \dots & \dots \\ 0 & 0 & 0 & \dots & T_0^{N_z-1} & 0 \end{bmatrix}; \mathbf{U_0}(\omega) = \begin{bmatrix} u_0^1 \\ u_0^2 \\ u_0^3 \\ \dots \\ u_0^{N_z} \end{bmatrix}; \mathbf{D}(\omega) = \begin{bmatrix} f\,d \\ 0 \\ 0 \\ \dots \\ 0 \end{bmatrix}$$

3

$$\mathcal{T}_0 = \begin{pmatrix} \mathbf{T_0}(\omega_1, \mathbf{s_0}) & 0 & \dots & 0 \\ 0 & \mathbf{T_0}(\omega_2, \mathbf{s_0}) & \dots & 0 \\ \dots & \dots & \dots & \dots \\ 0 & 0 & \dots & \mathbf{T_0}(\omega_{\mathbf{N}_\omega}, \mathbf{s_0}) \end{pmatrix}; \mathcal{U}_0 = \begin{pmatrix} \mathbf{U_0}(\omega_1) \\ \mathbf{U_0}(\omega_2) \\ \dots \\ \mathbf{U_0}(\omega_{\mathbf{N}_\omega}) \end{pmatrix}; \mathcal{D} = \begin{pmatrix} \mathbf{D}(\omega_1) \\ \mathbf{D}(\omega_2) \\ \dots \\ \mathbf{D}(\omega_{\mathbf{N}_\omega}) \end{pmatrix}$$

We can write the Equation (A-6) in matrix form as

$$\boxed{\mathcal{R}_0 = \mathcal{H}\mathcal{U}_0} \tag{A-7}$$

$$\begin{pmatrix} r_0^1 \\ r_0^2 \\ \dots \\ r_0^{N_z} \end{pmatrix} = \left(\begin{vmatrix} 1 & 0 & \dots & 0 \\ 0 & 1 & \dots & 0 \\ \dots & \dots & \dots & \dots \\ 0 & 0 & \dots & 1 \end{vmatrix} \begin{vmatrix} 1 & 0 & \dots & 0 \\ 0 & 1 & \dots & 0 \\ \dots & \dots & \dots & \dots \\ 0 & 0 & \dots & 1 \end{vmatrix} \begin{matrix} \dots \\ \dots \\ \dots \\ \dots \end{matrix} \begin{vmatrix} 1 & 0 & \dots & 0 \\ 0 & 1 & \dots & 0 \\ \dots & \dots & \dots & \dots \\ 0 & 0 & \dots & 1 \end{vmatrix} \right) \begin{pmatrix} \mathbf{U_0}(\omega_\mathbf{1}) \\ \mathbf{U_0}(\omega_\mathbf{2}) \\ \dots \\ \mathbf{U_0}(\omega_{\mathbf{N}_\omega}) \end{pmatrix}$$

where

- $\mathcal{H}$ is an operator performing the summation over frequency for every depth level z, and
- $\mathcal{R}_0$ is a column vector containing the image at every depth level. [4]

Therefore, the image ($\mathcal{R}_0$), corresponding to the background velocity field, can be computed from the measured data ($\mathcal{D}$) using the summation ($\mathcal{H}$) and the downward continuation operators ($\mathcal{T}_0$) as

$$\boxed{\mathcal{R}_0 = \mathcal{H}(\mathcal{I} - \mathcal{T}_0)^{-1}\mathcal{D}} \tag{A-8}$$

Adjoint operator: Modeling

Equation (A-8) enables us to compute the image corresponding to a given velocity field from data measured at the surface of the earth, that is, to migrate the data. The operation adjoint to migration, modeling, can be derived from the same equation using the adjoint state system

$$\overline{\mathcal{D}} = [\mathcal{H}(\mathcal{I} - \mathcal{T}_0)^{-1}]'\mathcal{R}_0 \tag{A-9}$$

where

- $\overline{\mathcal{D}}$ is the modeled data, computed for a given velocity field.

Therefore, we can obtain the modeled data ($\overline{\mathcal{D}}$) from the reflectivity image ($\mathcal{R}_0$) by writing

$$\boxed{\overline{\mathcal{D}} = \left[(\mathcal{I} - \mathcal{T}_0)^{-1}\right]' \mathcal{H}'\mathcal{R}_0} \tag{A-10}$$

---

[4]

$$\mathcal{H} = \left(\begin{vmatrix} 1 & 0 & \dots & 0 \\ 0 & 1 & \dots & 0 \\ \dots & \dots & \dots & \dots \\ 0 & 0 & \dots & 1 \end{vmatrix} \begin{vmatrix} 1 & 0 & \dots & 0 \\ 0 & 1 & \dots & 0 \\ \dots & \dots & \dots & \dots \\ 0 & 0 & \dots & 1 \end{vmatrix} \begin{matrix} \dots \\ \dots \\ \dots \\ \dots \end{matrix} \begin{vmatrix} 1 & 0 & \dots & 0 \\ 0 & 1 & \dots & 0 \\ \dots & \dots & \dots & \dots \\ 0 & 0 & \dots & 1 \end{vmatrix} \right); \mathcal{R}_0 = \begin{pmatrix} r_0^1 \\ r_0^2 \\ \dots \\ r_0^{N_z} \end{pmatrix}$$

APPENDIX B: FIRST-ORDER BORN LINEARIZATION OF MIGRATION

Forward operator: Perturbation migration

1. Scattering and downward continuation

   If we perturb the velocity model we introduce a perturbation in the wavefield. In other words, the perturbation in slowness generates a secondary wavefield, the scattered wavefield. We can downward continue the scattered field as we did with the background wavefield by writing

$$\boxed{\Delta u^{z+1}(\omega) = T_0^z(\omega, s_0)\Delta u^z(\omega) + \Delta v^{z+1}(\omega)} \tag{B-1}$$

   where

   - $\Delta u^z(\omega)$ is the perturbation in the wavefield generated by the perturbation in velocity, and
   - $\Delta v^{z+1}(\omega)$ represents the scattered wavefield caused at depth level $z+1$ by the perturbation in velocity from the depth level z.

   The scattered wavefield can be written as

$$\Delta v^{z+1}(\omega) = T_0^z(\omega, s_0)G_0^z(\omega, s_0)u_0^z(\omega)\Delta s^z(\omega) \tag{B-2}$$

   where

   - $G_0^z(\omega, s_0)$ is the scattering operator at depth z, and
   - $\Delta s^z(\omega)$ is the perturbation in slowness at depth z.

   Huang et al. (1999) show that the scattering operator is

$$G_0^z(\omega, s_0) = i\omega \frac{1}{\sqrt{1 - \frac{|\vec{k}|^2}{\omega^2 s_0^2}}} \tag{B-3}$$

   and that it can be approximated by

$$G_0^z(\omega, s_0) \approx i\omega \left(1 + \frac{1}{2}\frac{|\vec{k}|^2}{\omega^2 s_0^2}\right) \tag{B-4}$$

   which represents the first-order Born approximation. In this equation, $\vec{k}$ represents the horizontal component of the wavenumber.

   If we introduce Equation (B-2) into (B-1) we obtain

$$\Delta u^{z+1} = T_0^z \left[\Delta u^z + G_0^z u_0^z \Delta s^z\right] \tag{B-5}$$

which, after rearrangements, becomes the recursion

$$\Delta u^{z+1} - T_0^z \Delta u^z = T_0^z G_0^z u_0^z \Delta s^z \tag{B-6}$$

We can express the recursive relationship between the perturbation in velocity and the perturbation in the wavefield (B-6) as

$$\boxed{[\mathbf{I} - \mathbf{T_0}]\Delta\mathbf{U} = \mathbf{T_0}\mathbf{G_0}\widehat{\mathbf{U_0}}\Delta\mathbf{S}} \tag{B-7}$$

$$\begin{bmatrix} 1 & 0 & 0 & ... & 0 & 0 \\ -T_0^1 & 1 & 0 & ... & 0 & 0 \\ 0 & -T_0^2 & 1 & ... & 0 & 0 \\ ... & ... & ... & ... & ... & ... \\ 0 & 0 & 0 & ... & -T_0^{N_z-1} & 1 \end{bmatrix} \begin{bmatrix} \Delta u^1 \\ \Delta u^2 \\ \Delta u^3 \\ ... \\ \Delta u^{N_z} \end{bmatrix} = \begin{bmatrix} 0 & 0 & 0 & ... & 0 & 0 \\ T_0^1 & 0 & 0 & ... & 0 & 0 \\ 0 & T_0^2 & 0 & ... & 0 & 0 \\ ... & ... & ... & ... & ... & ... \\ 0 & 0 & 0 & ... & T_0^{N_z-1} & 0 \end{bmatrix} \begin{bmatrix} 0 & 0 & 0 & ... & 0 & 0 \\ G_0^1 & 0 & 0 & ... & 0 & 0 \\ 0 & G_0^2 & 0 & ... & 0 & 0 \\ ... & ... & ... & ... & ... & ... \\ 0 & 0 & 0 & ... & G_0^{N_z-1} & 0 \end{bmatrix} \begin{bmatrix} u_0^1 & 0 & 0 & ... & 0 \\ 0 & u_0^2 & 0 & ... & 0 \\ 0 & 0 & u_0^3 & ... & 0 \\ ... & ... & ... & ... & ... \\ 0 & 0 & 0 & ... & u_0^{N_z} \end{bmatrix} \begin{bmatrix} \Delta s^1 \\ \Delta s^2 \\ \Delta s^3 \\ ... \\ \Delta s^{N_z} \end{bmatrix}$$

where

- $\Delta\mathbf{U}$ is a column vector containing the perturbation in the wavefield at all depths,
- $\mathbf{G_0}$ is a diagonal matrix containing the scattering term for all the depth levels,
- $\widehat{\mathbf{U_0}}$ is a diagonal matrix containing the background wavefield data for all the depth levels, and
- $\Delta\mathbf{S}$ is a column vector containing the perturbation in the velocity for all the depth levels. [5]

Note the different arrangement of the background wavefield data at all depths ($\mathbf{U_0}$ and $\widehat{\mathbf{U_0}}$). [6]

Similarly to the case of the background wavefield, the relationship between the perturbation in the wavefield and the perturbation in slowness can be written for all the frequencies in the data as

$$\boxed{(\mathcal{I} - \mathcal{T}_0)\Delta\mathcal{U} = \mathcal{T}_0\mathcal{G}_0\widehat{\mathcal{U}_0}\Delta\mathcal{S}} \tag{B-8}$$

5

$$\Delta\mathbf{U} = \begin{bmatrix} \Delta u^1 \\ \Delta u^2 \\ \Delta u^3 \\ ... \\ \Delta u^{N_z} \end{bmatrix}; \mathbf{G_0} = \begin{bmatrix} 0 & 0 & 0 & ... & 0 & 0 \\ G_0^1 & 0 & 0 & ... & 0 & 0 \\ 0 & G_0^2 & 0 & ... & 0 & 0 \\ ... & ... & ... & ... & ... & ... \\ 0 & 0 & 0 & ... & G_0^{N_z-1} & 0 \end{bmatrix}; \widehat{\mathbf{U_0}} = \begin{bmatrix} u_0^1 & 0 & 0 & ... & 0 \\ 0 & u_0^2 & 0 & ... & 0 \\ 0 & 0 & u_0^3 & ... & 0 \\ ... & ... & ... & ... & ... \\ 0 & 0 & 0 & ... & u_0^{N_z} \end{bmatrix}; \Delta\mathbf{S} = \begin{bmatrix} \Delta s^1 \\ \Delta s^2 \\ \Delta s^3 \\ ... \\ \Delta s^{N_z} \end{bmatrix}$$

6

$$\mathbf{U_0} = \begin{bmatrix} u_0^1 \\ u_0^2 \\ u_0^3 \\ ... \\ u_0^{N_z} \end{bmatrix}; \widehat{\mathbf{U_0}} = \begin{bmatrix} u_0^1 & 0 & 0 & ... & 0 \\ 0 & u_0^2 & 0 & ... & 0 \\ 0 & 0 & u_0^3 & ... & 0 \\ ... & ... & ... & ... & ... \\ 0 & 0 & 0 & ... & u_0^{N_z} \end{bmatrix}$$

$$\begin{pmatrix} \mathbf{I}-\mathbf{T_0}(\omega_1,\mathbf{s_0}) & 0 & \dots & 0 \\ 0 & \mathbf{I}-\mathbf{T_0}(\omega_2,\mathbf{s_0}) & \dots & 0 \\ \dots & \dots & \dots & \dots \\ 0 & 0 & \dots & \mathbf{I}-\mathbf{T_0}(\omega_{\mathbf{N}_\omega},\mathbf{s_0}) \end{pmatrix} \begin{pmatrix} \Delta\mathbf{U}(\omega_1) \\ \Delta\mathbf{U}(\omega_2) \\ \dots \\ \Delta\mathbf{U}(\omega_{\mathbf{N}_\omega}) \end{pmatrix} = \begin{pmatrix} \mathbf{T_0}\mathbf{G_0}\widehat{\mathbf{U_0}}\Delta\mathbf{S}\Big|_{\omega_1} \\ \mathbf{T_0}\mathbf{G_0}\widehat{\mathbf{U_0}}\Delta\mathbf{S}\Big|_{\omega_2} \\ \dots \\ \mathbf{T_0}\mathbf{G_0}\widehat{\mathbf{U_0}}\Delta\mathbf{S}\Big|_{\omega_{\mathbf{N}_\omega}} \end{pmatrix}$$

where

- $\Delta\mathcal{U}$ is a column vector containing the perturbation in the wavefield for all the frequencies,
- $\mathcal{G}_0$ is a diagonal matrix containing the scattering operator for all the frequencies,
- $\widehat{\mathcal{U}_0}$ is a diagonal matrix containing the background wavefield for all the frequencies, and
- $\Delta\mathcal{S}$ is a column vector containing the perturbation in slowness, same for all the frequencies if we disregard dispersion. [7]

Again, it is important to note the different arrangement of the background wavefield data at all frequencies ($\mathcal{U}_0$ and $\widehat{\mathcal{U}_0}$). [8]

Therefore, we can compute the perturbation in the wavefield ($\Delta\mathcal{U}$) as a function of the perturbation in slowness ($\Delta\mathcal{S}$) like this:

$$\Delta\mathcal{U} = (\mathcal{I} - \mathcal{T}_0)^{-1}\mathcal{T}_0\mathcal{G}_0\widehat{\mathcal{U}_0}\Delta\mathcal{S} \tag{B-9}$$

2. Imaging

As for the background image, the perturbation in image (Δr^z), caused by the perturbation in slowness, is obtained by a summation over all the frequencies (ω):

$$\boxed{\Delta r^z = \sum_1^{N_\omega} \Delta u^z(\omega)} \tag{B-10}$$

We can write Equation (B-10) in matrix form as

$$\boxed{\Delta\mathcal{R} = \mathcal{H}\Delta\mathcal{U}} \tag{B-11}$$

$$\begin{pmatrix} \Delta r^1 \\ \Delta r^2 \\ \dots \\ \Delta r^{N_z} \end{pmatrix} = \left(\begin{vmatrix} 1 & 0 & \dots & 0 \\ 0 & 1 & \dots & 0 \\ \dots & \dots & \dots & \dots \\ 0 & 0 & \dots & 1 \end{vmatrix} \begin{vmatrix} 1 & 0 & \dots & 0 \\ 0 & 1 & \dots & 0 \\ \dots & \dots & \dots & 0 \\ 0 & 0 & \dots & 1 \end{vmatrix} \begin{matrix} \dots \\ \dots \\ \dots \\ \dots \end{matrix} \begin{vmatrix} 1 & 0 & \dots & 0 \\ 0 & 1 & \dots & 0 \\ \dots & \dots & \dots & \dots \\ 0 & 0 & \dots & 1 \end{vmatrix} \right) \begin{pmatrix} \Delta\mathbf{U}(\omega_1) \\ \Delta\mathbf{U}(\omega_2) \\ \dots \\ \Delta\mathbf{U}(\omega_{\mathbf{N}_\omega}) \end{pmatrix}$$

where

7

$$\Delta\mathcal{U} = \begin{pmatrix} \Delta\mathbf{U}(\omega_1) \\ \Delta\mathbf{U}(\omega_2) \\ \dots \\ \Delta\mathbf{U}(\omega_{\mathbf{N}_\omega}) \end{pmatrix}; \mathcal{G}_0 = \begin{pmatrix} \mathbf{G_0}(\omega_1,\mathbf{s_0}) & 0 & \dots & 0 \\ 0 & \mathbf{G_0}(\omega_2,\mathbf{s_0}) & \dots & 0 \\ \dots & \dots & \dots & \dots \\ 0 & 0 & \dots & \mathbf{G_0}(\omega_{\mathbf{N}_\omega},\mathbf{s_0}) \end{pmatrix}; \widehat{\mathcal{U}_0} = \begin{pmatrix} \widehat{\mathbf{U_0}}(\omega_1) & 0 & \dots & 0 \\ 0 & \widehat{\mathbf{U_0}}(\omega_2) & \dots & 0 \\ \dots & \dots & \dots & \dots \\ 0 & 0 & \dots & \widehat{\mathbf{U_0}}(\omega_{N_\omega}) \end{pmatrix}; \Delta\mathcal{S} = \begin{pmatrix} \Delta\mathbf{S} \\ \Delta\mathbf{S} \\ \dots \\ \Delta\mathbf{S} \end{pmatrix}$$

8

$$\mathcal{U}_0 = \begin{pmatrix} \mathbf{U_0}(\omega_1) \\ \mathbf{U_0}(\omega_2) \\ \dots \\ \mathbf{U_0}(\omega_{\mathbf{N}_\omega}) \end{pmatrix}; \widehat{\mathcal{U}_0} = \begin{pmatrix} \widehat{\mathbf{U_0}}(\omega_1) & 0 & \dots & 0 \\ 0 & \widehat{\mathbf{U_0}}(\omega_2) & \dots & 0 \\ \dots & \dots & \dots & \dots \\ 0 & 0 & \dots & \widehat{\mathbf{U_0}}(\omega_{N_\omega}) \end{pmatrix}$$

- $\Delta\mathcal{R}$ is a column vector containing the perturbation in image at every depth level z. [9]

Therefore, the perturbation in image ($\Delta\mathcal{R}$), corresponding to the perturbation velocity field ($\Delta\mathcal{S}$), can be computed as follows:

$$\boxed{\Delta\mathcal{R} = \mathcal{H}(\mathcal{I} - \mathcal{T}_0)^{-1}\mathcal{T}_0\mathcal{G}_0\widehat{\mathcal{U}_0}\Delta\mathcal{S}} \tag{B-12}$$

Adjoint operator: Back-projection

Equation (B-12) enables us to compute the perturbation in image corresponding to a given perturbation in the velocity field, that is, to migrate the scattered field. The operation adjoint to migration, back-projection, can be derived from the same equation using the adjoint state system:

$$\overline{\Delta\mathcal{S}} = \left[\mathcal{H}(\mathcal{I} - \mathcal{T}_0)^{-1}\mathcal{T}_0\mathcal{G}_0\widehat{\mathcal{U}_0}\right]' \Delta\mathcal{R} \tag{B-13}$$

where

- $\overline{\Delta\mathcal{S}}$ is the back-projected perturbation in the velocity field obtained from the perturbation in the image.

Therefore, the back-projected perturbation in velocity ($\overline{\Delta\mathcal{S}}$) is derived from the perturbation in the reflectivity image ($\Delta\mathcal{R}$) using the following expression:

$$\boxed{\overline{\Delta\mathcal{S}} = \widehat{\mathcal{U}_0}'\mathcal{G}_0'\mathcal{T}_0'\left[(\mathcal{I} - \mathcal{T}_0)^{-1}\right]'\mathcal{H}'\Delta\mathcal{R}} \tag{B-14}$$

Equations (B-12) and (B-14) comprise a pair of adjoint operators that relate the perturbation in velocity to the perturbation in reflectivity image. We can use these two operators to invert for velocity from measurable perturbations in the image.

9

$$\Delta\mathcal{R} = \begin{pmatrix} \Delta r^1 \\ \Delta r^2 \\ \cdots \\ \Delta r^{N_z} \end{pmatrix}$$